Uncertainty analysis methodology for multi-physics coupled rod ejection accident

G.-K Delipei, J. Garnier, J-C Le Pallec, B. Normand

UNCERTAINTY ANALYSIS METHODOLOGY FOR MULTI-PHYSICS COUPLED ROD EJECTION ACCIDENT

G.-K. Delipei[1], J. Garnier[2], J-C. Le Pallec[1] and B. Normand[1]
[1]: DEN - Service d'études des réacteurs et des mathématiques appliquées (SERMA)
CEA, Université Paris-Saclay, F-91191 Gif-Sur-Yvette, France

[2]: Centre de Mathématiques Appliquées
École Polytechnique, 91128 Palaiseau Cedex, France

gregory.delipei@cea.fr, josselin.garnier@polytechnique.edu,
jean-charles.le-pallec@cea.fr, benoit.normand@cea.fr

ABSTRACT

Nuclear reactor's transients computational modeling under an uncertainty framework creates many challenges related to the potential large number of inputs and outputs to be considered, their interactions and dependencies. In the particular case of Rod Ejection Accident (REA) in Pressurized Water Reactors (PWR) strong multi-physics coupling effects occur between neutronics, fuel-thermal and thermal-hydraulics. APOLLO3® neutronic code using two group diffusion modeling and FLICA4 thermal-hydraulic code using axial multi-channel 1D modeling are coupled in the framework of CORPUS Best Estimate multi-physics tool to model the REA. CORPUS, APOLLO3® and FLICA4 are developed at CEA and are used for the first time in a REA uncertainty analysis. Different statistical tools are explored and combined in an uncertainty analysis methodology using R language. The methodology is developed and tested on a small scale geometry representative of a PWR core. A total of 22 inputs are considered spanning neutronics, fuel-thermal and thermal-hydraulics. Three scalar and one functional outputs are studied. The methodology consists of different steps. First, a screening process based on dependence measures is performed in order to identify an important reduced input subspace. Second, a design of experiments is created by preserving good space-filling properties in both the original and reduced input spaces. This design is used to train kriging surrogate models only on the reduced subspaces. The kriging models are used then for brute force Monte Carlo (MC) uncertainty propagation and global sensitivity analysis by estimating Shapley indices. Concerning the functional output Principal Components Analysis (PCA) was used to reduce its dimension. The results show that the methodology manages to identify two subsets of important inputs and estimates the histograms and Shapley indices for both scalar and functional outputs. This will motivate the application of the derived methodology to a full core design for transient analysis purpose.

KEYWORDS: Multiphysics, REA, Uncertainty, Sensitivity, CORPUS, APOLLO3®, FLICA4

1. INTRODUCTION

Nuclear reactor's computational modeling and the related safety criteria lead towards Best Estimate Plus Uncertainty (BEPU) approaches. In BEPU the most important physical phenomena under both steady state and transient situations are represented under a probabilistic framework. Various sources of uncertainties related either to natural variability of physical quantities or to the modeling must be identified and taken into account. In the particular case of Rod Ejection Accident (REA) in Pressurized

Water Reactors (PWR) strong multi-physics coupling effects occur between neutronics, fuel-thermal and thermal-hydraulics. This necessitates a multi-physics modeling to take into account the interdisciplinary interactions increasing the computational cost. The uncertainty analysis for REA becomes thus very challenging. In a previous work we defined an approach with different coupling studies from separate physics to full coupling [1]. In this work we explore different statistical tools and combine them in an uncertainty analysis methodology using R language. The methodology is developed and tested on a small scale geometry representative of a PWR reactor. CORPUS Best Estimate multi-physics coupling tool developed at CEA [2] is used to couple APOLLO3® [3] and FLICA4 [4] CEA codes for the first time in a REA uncertainty analysis.

2. CASE STUDY

The REA is initiated by a control rod ejection due to mechanical malfunction inserting positive reactivity in the core. As a consequence power increases adiabatically until the fuel temperature starts increasing as well introducing a Doppler negative feedback that creates a power peak. The power then continues to decrease and when the heat flux reaches the moderator its density will start decreasing adding another negative feedback due to the negative moderator temperature effect. Depending on the core state at the moment of the ejection the power evolution and its damage on the first containment barrier (cladding) can vary significantly.

2.1. Geometry and modeling

The development of the uncertainty analysis methodology for REA is performed on a small scale geometry representative of a PWR consisting of 3x3 fuel assemblies with three different burn-up states (0, 15 and 30 GWd/t) and one ring of reflector assemblies in the periphery. Such a design, with its small computational time compared to a full core one, is suited for methodological exploration. The control rod is inserted in the central assembly and the core is rendered critical by boron concentration adjustment. The fission poisons follow an axial profile peaked towards the bottom of fuel assemblies, creating a corresponding power peak in the top part. This increases the control rod worth and thus the inserted reactivity. At the initial state the core is at hot zero power (HZP conditions). The control rod is ejected in 0.1s and we model the first 0.4s of the transient. The inserted reactivity at the reference case is 1.7$ leading to a prompt neutron driven transient. The geometry together with the reference power and the 3D deformation factor evolution in time are shown in figure 1. APOLLO3® two group diffusion is used on the 3D geometry for neutronics while FLICA4 axial multi-channel (1D) is used for thermal-hydraulics. For fuel-thermal the radial 1D model of FLICA4 with constant pellet/cladding gap heat transfer is used. The selected discretization level consists of 30 axial meshes and 4 radial per assembly. One thermal-hydraulic channel is considered per quarter of assembly and one average fuel pin per channel.

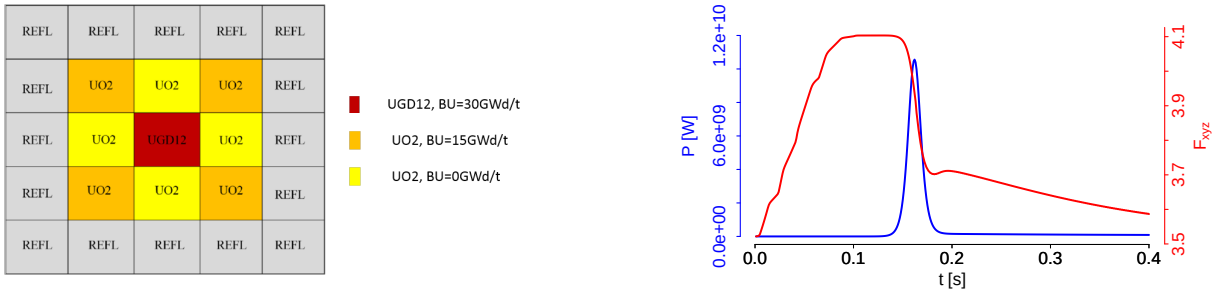

Figure 1: Geometry, reference power ($\mathbf{P}$) and 3D deformation factor ($\mathbf{F_{xyz}}$) evolution in time for the studied scenario

2.2. Inputs-Outputs identification

For this modeling the uncertain inputs and outputs that will be considered are identified by discipline and presented in table 1. We selected 22 scalar inputs, 3 scalar and 1 functional outputs.

Table 1: Inputs and outputs identification by discipline: **neutronics**, **fuel-thermal** and **thermal-hydraulics**.

Inputs (22)			
$\mathbf{TD_g(2)}$	Disappearance cross-section of group g	$\mathbf{NF_g(2)}$	νxfission cross-section of group g
$\mathbf{D_g(2)}$	Diffusion coefficient of group g	$\mathbf{S_{1\to 2}}$	Scattering cross-section of group 1 to 2
$\mathbf{IV_g(2)}$	Inverse velocity of group g	$\beta_{\mathbf{eff}}$	Effective delayed neutrons
$\lambda_{\mathbf{eff}}$	Effective decay constant		
$\lambda_{\mathbf{f}}$	Fuel thermal conductivity	$\lambda_{\mathbf{c}}$	Cladding thermal conductivity
$\mathbf{Cp_f}$	Fuel specific heat capacity	$\mathbf{Cp_c}$	Cladding specific heat capacity
$\mathbf{H_{gap}}$	Fuel-cladding gap heat transfer	$\mathbf{T_R}$	Rowland temperature
$\mathbf{P_r}$	Power radial profile		
$\mathbf{H_c}$	Convective heat transfer	$\mathbf{R_{crit}}$	Criterion for post-DNB heat transfer
$\mathbf{R_{v0}}$	Recondensation	$\mathbf{H_{dnb}}$	Post-DNB heat transfer
Outputs (3 scalars + 1 functional)			
$\mathbf{P_{lin}^{max}}$	Local linear power (max in time)	$\mathbf{P_{lin}^{2D}(x,y)}$	Radial distribution of linear power at the time and axial position of $\mathbf{P_{lin}^{max}}$
$\mathbf{H_f^{max}}$	Fuel stored enthalpy (max in time)		
$\mathbf{DNB^{min}}$	Distance from $\mathbf{R_{crit}}$ (min in time)		

The neutronics uncertainties are quantified by a multivariate Gaussian distribution using an empirical covariance matrix estimated by neutronic lattice uncertainty propagation results provided by the OECD international activity UAM [5]. The fuel-thermal and thermal-hydraulics uncertainties are quantified using UAM recommendations wherever possible and expert opinions for the rest. Their probability distributions together with the UAM correlation matrix for neutronics can be seen in figure 2.

Fuel-thermal	
$\lambda_{\mathbf{f}}$	N(1,0.05)
$\lambda_{\mathbf{c}}$	N(1,0.05)
$\mathbf{Cp_f}$	N(1,0.05)
$\mathbf{Cp_c}$	N(1,0.05)
$\mathbf{H_{gap}}$	U(2000,50000)
$\mathbf{P_r}$	U(0,0.04) + N(0,0.0175)
$\mathbf{T_R}$	U(0,1)
Thermal-hydraulics	
$\mathbf{H_c}$	N(1,0.15)
$\mathbf{R_{crit}}$	N(1,0.15)
$\mathbf{R_{v0}}$	N(1,0.125)
$\mathbf{H_{dnb}}$	U(0.8,1.2)

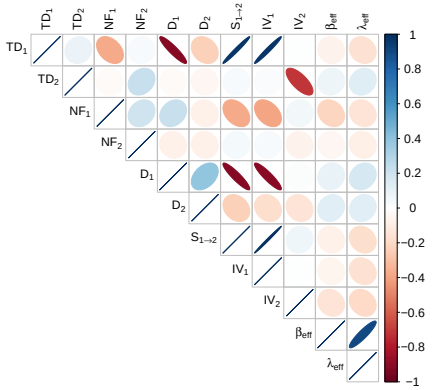

Figure 2: Inputs uncertainty quantification, where U(a,b) is a uniform distribution over (a,b) and N(a,b) is a normal distribution with mean a and standard deviation b.

3. UNCERTAINTY ANALYSIS METHODOLOGY

The general uncertainty analysis methodology is essentially based on [6] and [7] and is synthetically presented in figure 3. The final goals are to propagate the uncertainties to the outputs of interest by estimating their histograms and perform a global sensitivity analysis. Both of them demand a large number of code evaluations (10^5) that cannot be practically performed, in most of the cases, directly by using the code. To overcome this limitation the underlying function between each output and the inputs is approximated by a kriging surrogate model. Kriging models must be trained and evaluated on designs of experiments (DOE) that explore the input space as efficiently as possible. These designs are called space-filling designs. We use Latin Hypercube Sampling (LHS) with optimization by maximizing the minimum distance between the design points. The training of the surrogate models for large input dimensions can be difficult. There is thus a strong interest in identifying a reduced input subspace that explains most of the output's variation. This subset is identified with an initial random sampling exploring the complete

input space. Two methods can be used to reduce the input dimension. The first one is the Principal Components Analysis (PCA). It identifies linear projections of the inputs that represent most of their variations based on their empirical correlations. It is well adapted for functional inputs or outputs. The second one is a screening method estimating the statistical significance of each input to each output by using Hilbert-Schmidt Independence Criterion (HSIC) dependence measures. While in cases of very large input dimension the combination of both was developed, in this work we limit the HSIC to the input dimension reduction and the PCA to the functional output dimension reduction. The different statistical tools together with the inputs dimension reduction and the functional output treatment will be detailed in the following paragraphs. To this purpose we define the function $\mathbf{Y} = F(\mathbf{X}) : \mathbb{R}^d \rightarrow \mathbb{R}^q$ to be the underlying function between the random inputs of dimension d and random scalar ($q = 1$) or functional ($q >> 1$) output. We consider to have obtained a dataset of N realizations of $\left[\mathbf{X}_n, \mathbf{Y}_n = F(\mathbf{X}_n)\right]_{n=1}^{N}$. The nth realization of ith input is denoted by X_n^i.

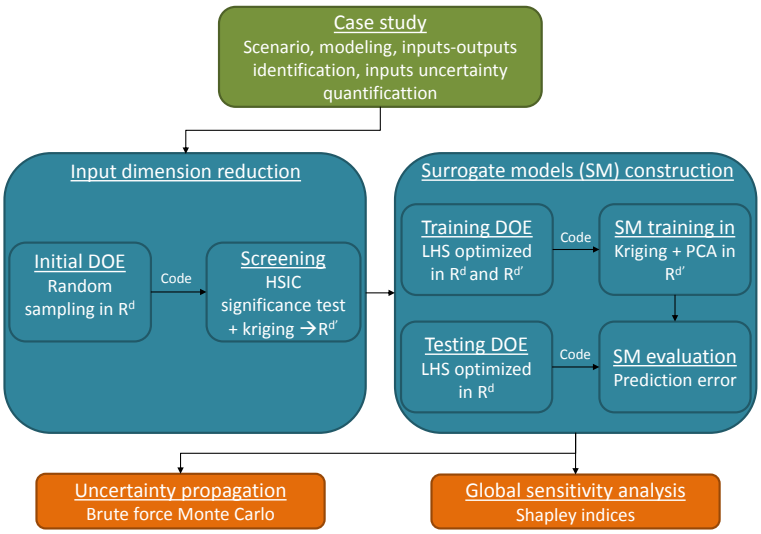

Figure 3: UAM methodology with d the original input space dimension and d' the reduced input space dimension.

3.1. HSIC independence test

The screening process needs to identify with few code evaluations the sensitivity between inputs and outputs including potential non-linearities. To this purpose we use the HSIC dependence measures [7]. In general the dependence measure aims at estimating the effect of each input on the whole distribution of the outputs. We consider one input $X^i \in \mathbb{R}_x$ and a scalar output $Y \in \mathbb{R}_y$. We associate to X^i the universal Reproducing Kernel Hilbert-Schmidt (RKHS) function space $\mathcal{F}_x$ mapping $\mathbb{R}_x$ to $\mathbb{R}$. The inner product in this space for an arbitrary function $f_x \in \mathcal{F}_x$ can be computed through a unique positive definite kernel $k_x : \mathbb{R}_x \times \mathbb{R}_x \rightarrow \mathbb{R}$ by $< f_x(X^i), f_x(X^{i'}) >_{\mathcal{F}_x} = k_x(X^i, X^{i'})$. For the output Y we associate in an equivalent way the $\mathcal{F}_y$ RKHS function space and its corresponding kernel $k_y : \mathbb{R}_y \times \mathbb{R}_y \rightarrow \mathbb{R}$. With theses definitions the linear operator of cross covariance C_{X^iY} between X^i and Y takes the form of equation 1 (left). Finally, the Hilbert-Schmidt Independence Criterion (HSIC) is defined as the Hilbert-Schmidt norm of this operator and can be estimated empirically through equation 2. The use of non linear kernels generalizes the covariance of (X^i, Y).

$$< f_x, C_{X^iY} f_y >_{\mathcal{F}_x} = Cov(f_x(X^i), f_y(Y)) \quad , \quad HSIC(X^i, Y) = \|C_{X^iY}\|_{HS}^2 \tag{1}$$

$$\widehat{HSIC}(X^i, Y) = \frac{Tr(\mathbf{K}_x \mathbf{H} \mathbf{K}_y \mathbf{H})}{N^2} \tag{2}$$

Where $\mathbf{K}_x$ and $\mathbf{K}_y$ are the Gram matrices of the kernel functions defined as $K_x^{jk} = k_x(X_j^i, X_k^i)$ and $K_y^{jk} = (k_y(Y_j, Y_k))$ for $j \leq N, k \leq N$. $\mathbf{H}$ is a centering matrix with elements $H^{jk} = \delta_{jk} - \frac{1}{N}$ for $j \leq N, k \leq N$. There is no clear way for the selection of the kernel functions. For this work Gaussian kernels were selected using the empirically estimate variance of each random variable. While the HSIC indices measure non-linear dependencies between X^i and Y they are not robust enough to be used directly for screening. It is preferable that they are used in significance tests. The non-asymptotic significant test based on resampling presented in [7] is used for screening purposes. The null hypothesis "$H_0 : X^i$ and Y are independent" is adopted with a significance level $\alpha = 0.05$. The following procedure is applied for each input to identify which of them are important.

HSIC significance test

1: Initialize $\alpha = 0.05$, B bootstrap size and $p = 0$
2: Compute $\widehat{HSIC}(X^i, Y)$
3: Realize B bootstrap samples Y^b of Y
4: **for** $(b = 1, b \leq B, b++)$ **do**
5: Compute HSIC indice between X^i and Y^b: $\widehat{HSIC}(X^i, Y^b)$
6: $p = p + \frac{1}{B} 1_{\widehat{HSIC}(X^i,Y^b) > \widehat{HSIC}(X^i,Y)}$
7: If $p < \alpha$ the H_0 is rejected and the variable X^i is considered important for Y

3.2. Kriging

Kriging surrogate model uses Gaussian processes to approximate the scalar function $Y = F(\mathbf{X})$ with $F(\mathbf{X}) = \mu(\mathbf{X}) + Z(\mathbf{X})$, where $\mu(\mathbf{X})$ is a mean function and $Z(\mathbf{X})$ is a centered Gaussian process. The covariance function of $Z(\mathbf{X})$ is considered stationary $k(\mathbf{X}_1, \mathbf{X}_2) = \sigma^2 \prod_{i=1}^{d} k_{\theta_i}(|X_1^i - X_2^i|)$ with $k_{\theta_i}(0) = 1$, where $\mathbf{X}_1, \mathbf{X}_2$ are two design points. The variance σ^2 is constant and must be estimated. The covariance function is a positive definite function and is selected from specific families of parametric functions (e.g. Exponential, Matérn). In this work we used the Matérn 5/2 function. The selected covariance function has d hyper-parameters $\boldsymbol{\theta}$ to be estimated representing the correlation length associated to each input. Universal Kriging is used and the mean function is a linear combinations of inputs $\mu(\mathbf{X}) = (\frac{1}{\mathbf{X}})^T \boldsymbol{\beta}$. The unknown vector of coefficients $\boldsymbol{\beta}$ of size $d + 1$ must be estimated as well. The vector parameters $(\boldsymbol{\theta}, \sigma, \boldsymbol{\beta})$ is estimated by Maximum Likelihood [8]. The dataset of size N is used as a training DOE and we denote by $\mathbf{X}_{doe}$ and $\mathbf{Y}_{doe}$ the input matrix of size $N \times d$ and the output vector of size N respectively. Conditioning on this dataset, the expected value of a new prediction $\hat{Y}_{new}$ for $\mathbf{X}_{new}$ and its associated variance are given by equations 3 and 4.

$$\hat{Y}_{new} = \mu(\mathbf{X}_{new}) + \mathbf{k}(\mathbf{X}_{new})^T \mathbf{K}^{-1} (\mathbf{Y}_{doe} - \mathbf{M}_{doe}) \tag{3}$$

$$\hat{\sigma}^2_{new} = \hat{\sigma}^2 - \mathbf{k}(\mathbf{X}_{new})^T \mathbf{K}^{-1} \mathbf{k}(\mathbf{X}_{new}) + \mathbf{B}^T \left(\mathbf{X}_{doe}^T \mathbf{K}^{-1} \mathbf{X}_{doe} \right)^{-1} \mathbf{B} \tag{4}$$

In the above equations $\mathbf{B} = \mathbf{X}_{new} - \mathbf{X}_{doe}^T \mathbf{K}^{-1} \mathbf{k}(\mathbf{X}_{new})$. The estimated hyperparameters are $\hat{\boldsymbol{\beta}}$, $\hat{\boldsymbol{\theta}}$ and $\hat{\sigma}$. $\mathbf{M}_{doe}$ is the mean vector on the dataset with elements $M^j = \mu(\mathbf{X}_j)$ for $j \leq N$. The vector $\mathbf{k}(\mathbf{X}_{new})$ of size N is defined as $k^j = k(\mathbf{X}_{new}, \mathbf{X}_j)$ for $j \leq N$. $\mathbf{K}$ is a $N \times N$ covariance matrix with $K^{jk} = k(\mathbf{X}_j, \mathbf{X}_k)$ for $j \leq N, k \leq N$. The approximation of $Y = F(\mathbf{X})$ by a kriging model induces an error for the future predictions. The estimation of this error is done by an independent DOE on which the code is evaluated and the results are compared with the kriging predictions. The ratio of the variance of this discrepancies with the empirical variance of the output is the relative prediction error. If an evaluation DOE is not available the leave-one-out error (LOO) is used as an estimation of the error. This error estimation is computed by calculating for each point in the dataset the discrepancy with the prediction of a kriging model constructed using all the other points. Again the ratio of the variance of theses discrepancies with the empirical variance is the relative LOO error.

3.3. Optimized LHS

The LHS is optimized based on space-filling criteria. From the various existing methods the simulated annealing is used. The optimization consists of maximizing the minimum distance between the design points. This is achieved by minimizing the criterion ϕ_p, defined by using the euclidean distance between two design points $d_{jk} = \|\mathbf{X_j} - \mathbf{X_k}\|_2$.

$$\phi_p = \Big[\sum_{j,k \leq N,\, j<k} d_{jk}^{-p} \Big]^{\frac{1}{p}} \tag{5}$$

A value of $p = 50$ was used as in [9]. For the kriging model training and evaluation two independent LHS are constructed. The first one is used for the training on the reduced input subspace. It is important that it has good space-filling properties in this subspace. With this in mind we adapted the optimization process of LHS in order to optimize in both the complete and reduced input spaces. This will allow to include in the kriging models prediction error the error due to the inputs dimension reduction.

3.4. Shapley indices

This global sensitivity analysis method was developed quite recently [10] and it can be seen as a generalization of Sobol indices that can treat dependent input parameters. They are based on game theory and the main idea is to calculate the impact of an input on the output for all its possible combinations with the other inputs. In order to estimate the Shapley indices we will introduce some definitions. Considering the inputs $\mathbf{X}$ and the scalar output Y we define $K = \{1, 2, \ldots, d\}$ the set containing all the indices of the inputs parameters, π a permutation of the indices in K and $P_i(\pi)$ as the set that includes all parameters preceding index i in π. For example if $d = 6$ then $K = \{1, 2, 3, 4, 5, 6\}$, π could be $\{3, 6, 2, 1, 5, 4\}$ and then $P_1(\pi) = \{3, 6, 2\}$. The next step now is to define a cost function that relates a set of parameters to a value. In the context of global sensitivity the selected function is:

$$c(J) = E[Var(Y|\mathbf{X}^{\sim J})] \tag{6}$$

With $J \subseteq K$ and $\mathbf{X}^{\sim J} = (X^i)_{i \in K \setminus J}$ the complement of $\mathbf{X}^J$. The $c(J)$ cost function is interpreted as the expected remaining output variance if all the parameters except the ones in J are known. If we define $\Pi(K)$ the set of all possible perturbations of K then the exact Shapley index for the input X^i is the one in equation 7.

$$Sh_i = \sum_{\pi \in \Pi(K)} \frac{1}{d!} (c(P_i(\pi) \cup \{i\}) - c(P_i(\pi))) \tag{7}$$

The cost function can be estimated by two loop Monte Carlo simulations [10]. The number of possible permutations increases factorialy with the dimension of the inputs vector. To overcome this limitation M random permutations π_r are generated and an approximate Shapley index is calculated by equation 8.

$$\widehat{Sh}_i = \frac{1}{M} \sum_{r=1}^{M} (\hat{c}(P_i(\pi_r) \cup \{i\}) - \hat{c}(P_i(\pi_r))) \tag{8}$$

3.5. Principal Components Analysis (PCA)

We consider the functional output $\mathbf{Y}$, which means that Y is $\mathbb{R}^q$-valued with $q >> 1$. From the collected N evaluations $\mathbf{Y}_N$ in a $N \times q$ matrix the empirical mean is estimated $\hat{\boldsymbol{\mu}}_{\boldsymbol{Y}}$ and extracted to create the centered around zero matrix $\mathbf{Y}_{c,N}$. PCA is an orthogonal linear transformation of $\mathbf{Y}_{c,N}$ where each principal component represents in a descending order parts of variance [11]. If $\mathbf{Y}_{c,N}$ has strong correlations, as in the case of spatial fields, the number of principal components needed to represent 99% of

the variance can be quite small. This is carried out by first computing the empirical covariance matrix and its eigenvalue decomposition. The $q \times q$ matrix $\mathbf{W}$ contains the eigenvectors, with ith eigenvector at the ith column, and the $q \times q$ diagonal matrix $\mathbf{\Lambda}$ contains the eigenvalues with the ith one on Λ_{ii}. The transformed coordinates of the original quantity are called scores and stored in $\mathbf{T}$.

$$\mathbf{C} = \frac{\mathbf{Y}_{c,N}^T \mathbf{Y}_{c,N}}{N}, \quad \mathbf{C} = \mathbf{W}\mathbf{\Lambda}\mathbf{W}^{-1}, \quad \mathbf{T} = \mathbf{Y}_{c,N}\,\mathbf{W} \tag{9}$$

The principal components eigenvalues are in a descending order of variance explanation. By discarding the eigenvectors with eigenvalues below a threshold L and the corresponding scores, the output space can be significantly reduced. When there is the need to calculate the original output an approximation of it $\tilde{\mathbf{Y}}_N$ can be calculated by the truncated matrices $\mathbf{T_L}$ ($N \times L$), $\mathbf{W_L}$ ($q \times L$) and the extracted mean function through $\tilde{\mathbf{Y}}_N = \mathbf{T_L}\mathbf{W_L}^T + \mathbf{M_Y}$. The matrix $\mathbf{M_Y}$ of size $N \times q$ contains $\hat{\boldsymbol{\mu}}_{\boldsymbol{Y}}$ at each row. In a similar way new output predictions can be made if a surrogate model is constructed between the inputs and the scores.

3.6. Input dimension reduction method

As mentioned the dimension of the input space is large and potentially only a small subspace is important for a scalar output Y. The goal of this method is to identify this important input subspace. We denote by $\mathcal{S}_d$ the set of size d containing the inputs indices and $\mathbf{X}_d$ the corresponding inputs. There are many challenges related to the dependencies between inputs, potential interactions, redundancies and the non-linear behavior between inputs and outputs. There is no methodology that can deal efficiently with all of theses constraints. In this work we use the HSIC significance tests to treat dependencies, non-linearities and interactions. The results is an initial subset of inputs considered as important ($\mathcal{S}_{d0}$, $\mathbf{X}_{d0}$). Using this subset a kriging model (Kr) is trained and its LOO error is estimated (ϵ_{LOO}). If the error is not satisfactory, inputs are sequentially added until the user decides to stop or until all the inputs are included ($\mathcal{S}_{d1}$, $\mathbf{X}_{d1}$). This is applicable to our case of 22 inputs but it can be prohibitive for much larger inputs cases. Finally, in order to treat the redundancies, the resulting subspace from the previous step is subjected to a sequential extraction of one input at a time and the corresponding LOO error is computed. If the error stays close to constant within a small $\delta\varepsilon$ when the input is extracted then the input is rejected from the subspace ($\mathcal{S}_{d2}$, $\mathbf{X}_{d2}$). This step has to be used with caution, it can reduce the inputs subspace in term of representation but still the correlated rejected inputs should be mentioned. This input dimension reduction method is carried out with an initial random DOE. The following procedure details the input dimension reduction process. The inputs $\mathbf{X}_{di}$ are defined by the set of indices $\mathcal{S}_{di}$.

Input dimension reduction process

Code evaluations on initial random DOE.
HSIC significance test $\rightarrow$ initial important subspace $\mathcal{S}_{d0}$ and $\mathbf{X}_{d0} \in \mathbb{R}^{d0}$
Compute ϵ_{LOO} for Kr($\mathbf{X}_{d0}, Y$), set $\mathcal{S}_{r0}$ as the rejected inputs subspace of size $r0 = d - d0$ and $\mathcal{S}_{d1} = \mathcal{S}_{d0}$
while User decision based on error evolution **do**
    for ($i = 1, i \leq r0, i++$) **do**
        Compute ϵ^i_{LOO} for Kr($\mathbf{X}_{d1} \cup X^i_{r0}, Y$)
    Selection of X^i_{r0} and its corresponding index S^i_{r0} with minimum ϵ^i_{LOO}
    Update $\mathcal{S}_{d1} = \mathcal{S}_{d1} \cup \mathcal{S}^i_{r0}$
Set $\mathcal{S}_{d2} = \mathcal{S}_{d1}$, update ϵ_{LOO} for Kr($\mathbf{X}_{d1}, Y$) and define error threshold $\delta\epsilon$
for ($i = 1, i \leq d2, i++$) **do**
    Compute ϵ^i_{LOO} for Kr($\mathbf{X}_{d2,i}, Y$) with $\mathbf{X}_{d2,i}$ the inputs corresponding to $\mathcal{S}_{d2,i} = \mathcal{S}_{d2} \setminus \mathcal{S}^i_{d2}$
    if ($\epsilon^i_{LOO} - \epsilon_{LOO} < \delta\epsilon$) **then**
        $\mathcal{S}_{d2} = \mathcal{S}_{d2,i}$
Set of reduced inputs subspaces S_{d2} and the corresponding inputs $X_{d2} \in \mathbb{R}^{d2}$

3.7. Functional output treatment

The $\mathbb{R}^q$-valued functional output $\mathbf{Y}$ is subjected to PCA in order to reduce its analysis to a few scalar quantities. Based on the training DOE kriging models are used to approximate the underlying functions between the scalar PCA scores and the inputs. This enables the fast evaluation of new inputs points and by using brute Monte Carlo the inputs uncertainties are propagated to $\mathbf{Y}$. For the global sensitivity analysis the Shapley indices for the scores are estimated $\widehat{Sh}_i^l$, with $l \leq L$, for each input i. An aggregated index is computed through equation 10 weighted by the scores variance representation $V^l = \frac{\Lambda_{ll}}{Tr(\mathbf{\Lambda})}$ over the total variance of the functional output.

$$\widehat{Sh}_i^Y = \sum_{l=1}^{L} \widehat{Sh}_i^l V^l \tag{10}$$

4. RESULTS

4.1. Input dimension reduction

For the input dimension reduction process a random DOE of size 125 was used. The results for all the outputs lead to the identification of two important subspaces. The first one for the output DNB^{min} consists of $\beta_{eff}, Cp_c, H_{gap}, T_R$. The second one for the rest outputs (P_{lin}^{max}, H_f^{max}, $\mathbf{P_l^{2D}in}$) consists of $TD_1, NF_1, NF_2, D_1, S_{1\to2}, \beta_{eff}, Cp_f, H_{gap}$ and T_R. The construction of the LHS of size 250 for the kriging models training is improved by optimizing in theses subspaces. This results in a gain for the space-filling criterion ϕ_p that is visualized in figure 4. The evolution of ϕ_p is illustrated along the iterations of the optimization in the complete ($d = 22$) and the first important ($d = 4$) input spaces. The constructed LHS optimized in 22 dimensions and improved in 4 is compared to a LHS optimized only in 22 dimensions and another one optimized only in 4 dimensions. It is clear that we obtain a gain in space-filling properties that could enhance the predictive capabilities of the kriging model.

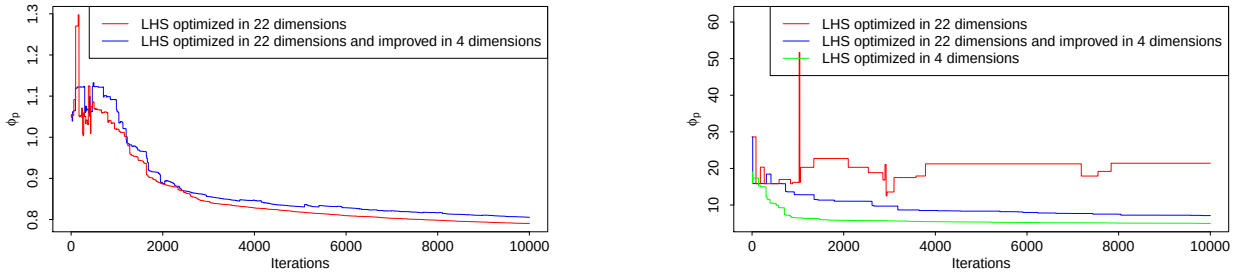

Figure 4: Space-filling criterion ϕ_p optimization in both the complete (left) and important inputs space (right).

4.2. Uncertainty propagation and global sensitivity analysis

The Kriging models were trained on the previous LHS and evaluated by a second LHS optimized only in the complete inputs space. The results show very small prediction errors. For P_{lin}^{max} and H_f^{max} the relative prediction error is 0.08% while for DNB^{min} is 1.44%. For the functional output of size $q = 36$ only two principal components are needed to represent 99% of its variance. The relative prediction errors for the the first two components are 0.08% and 0.44% respectively. The constructed kriging models are used in brute force Monte Carlo simulations to estimate the histograms of the outputs. The results are presented in figures 5 (scalar outputs) and 6 (functional output). The random output P_{lin}^{max} has a relative standard deviation of 23% and the histogram is close to Gaussian. The random output H_f^{max} has a Gaussian histogram with 13% relative standard deviation. The random output DNB^{min} is strongly non Gaussian with large relative standard deviation of 76% and a small probability of reaching

DNB conditions ($DNB^{min} < 0$). The functional $\mathbf{P_{lin}^{2D}}$ shows similar histograms to P_{lin}^{max} with relative standard deviation that do not vary significantly on the radial plane.

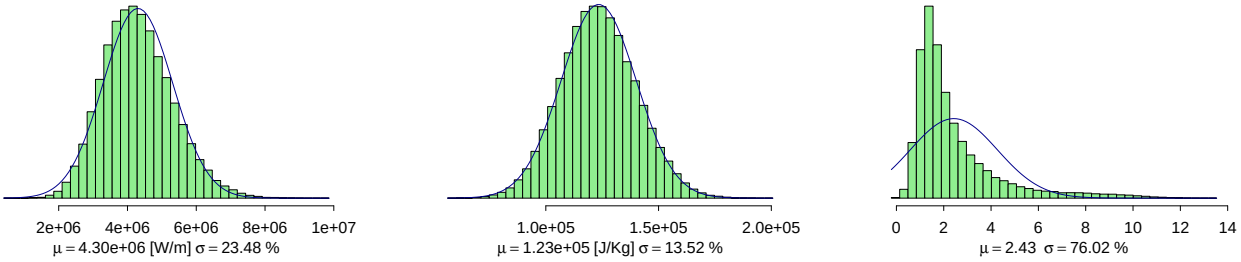

Figure 5: Estimated histograms of P_{lin}^{max} (left), H_f^{max} (center) and DNB^{min} (right)

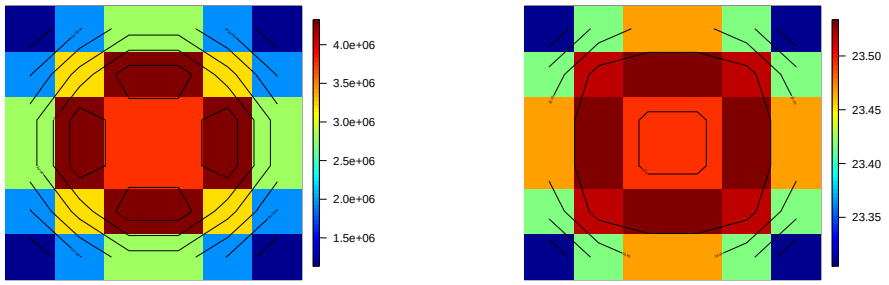

Figure 6: Mean in [W/m] (left) and relative standard deviation in [%] (right) for $\mathbf{P_{lin}^{2D}}$

The obtained outputs distributions are sensible to specific inputs. Theses sensibilities are captured by Shapley indices presented in figure 7. The results show that the effective delayed neutrons are the most dominant inputs for P_{lin}^{max}, H_f^{max} and $\mathbf{P_{lin}^{2D}}$. The gap heat transfer is the most important for the DNB^{min} which can be related to its constant value with a large range of variation imposed in the inputs uncertainty quantification.

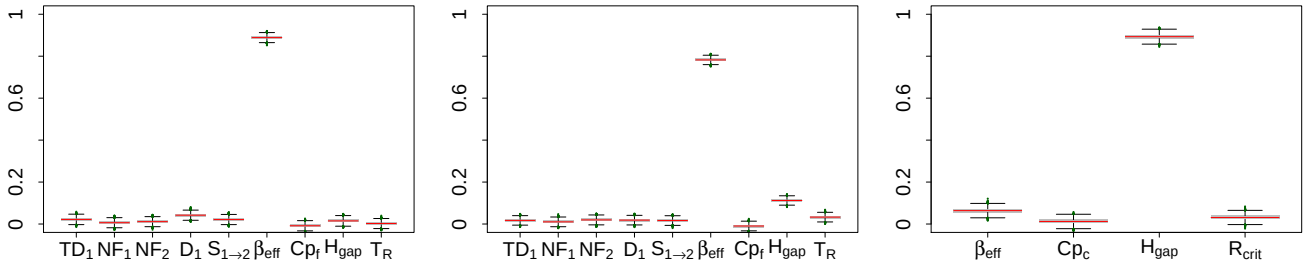

Figure 7: Shapley indices for P_{lin}^{max} and $\mathbf{P_{lin}^{2D}}$ (left), H_f^{max} (center) and DNB^{min} (right).

5. CONCLUSIONS

We developed and tested an uncertainty analysis methodology using R language that can treat large number of potential dependent inputs and scalar and functional outputs on a multi-physics REA modeled with CORPUS multi-physics coupling tool. An APOLLO3®-FLICA4 coupling on a small scale core representative of a PWR reactor was used. A total of 22 inputs were considered spanning neutronics, fuel-thermal and thermal-hydraulics. Three scalar and one functional outputs were studied. The scalar ones are the maximum local linear power, the maximum local stored enthalpy and the difference between the DNBR and the DNB criterion. The functional one is the radial linear power map at the time and axial position of maximum local linear power. The methodology initially identifies two important reduced input subspaces based on HSIC siginificance tests. A LHS is created by preserving good space-filling properties in both the original and reduced input spaces. This design is used to train kriging surrogate

models on the reduced subspaces. The kriging models are used for brute force Monte Carlo uncertainty propagation and global sensitivity analysis by estimating Shapley indices. Concerning the functional output PCA is used to reduce its dimensions. Two principal components are needed for representing 99% of the output's variance and aggregated Shapley indices are estimated. The results show that the effective delayed neutron fraction and the gap heat transfer are the most important inputs. All this work can be seen as a proof of concept for the developed methodology. The short term perspectives is to apply this methodology to a full core design submitted to REA including a calibration of a gap heat transfer model to better quantify its uncertain behavior.

ACKNOWLEDGEMENTS

APOLLO3® is registered trademark of CEA. We gratefully acknowledge CEA, Framatome, and EDF for their long-term partnership and support. We would like also to thank the APOLLO3® and FLICA4 development teams for their support and successful exchanges.

REFERENCES

[1] G.-K. Delipei, J. Garnier, J-C. Le Pallec, B.Normand. Multi-physics uncertainties propagation in a PWR Rod Ejection Accident modeling - Analysis methodology and first results. ANS Best Estimate Plus Uncertainty International Conference, Lucca, Italy, May 2018.

[2] J.-C. Le Pallec, K. Mer-Nkonga. Neutronics/Fuel Thermomechanics coupling in the framework of a REA (Rod Ejection Accident) Transient Scenario Calculation. PHYSOR 2016 Conference: Unifying Theory and Experiments in the 21st Century, Sun Valley, Idaho, USA, May 1-5, 2016.

[3] D. Schneider et al.. APOLLO3®: CEA/DEN deterministic multi-purpose code for reactor physics analysis. PHYSOR 2016, Sun Valley, Idaho, USA, May 1-5, 2016

[4] I. Toumi et al.. FLICA4: a three dimensional two-phase flow computer code with advanced numerical methods for nuclear applications. Nuclear Engineering and Design, 200:139-155, 2000.

[5] K. Ivanov, M. Avramova, S. Kamerow, I. Kodeli, E. Sartori, E. Ivanov and O. Cabellos. Benchmarks for uncertainty analysis in modelling (UAM) for the design, operation and safety analysis of LWRs". Volume I: Specification and Support Data for Neutronics Cases (Phase I), NEA/NSC/DOC(2013)7.

[6] B. Iooss and A. Marrel. Advanced Methodology for Uncertainty Propagation in Computer Experiments with Large Number of Inputs. Nuclear Technology, 1-19, March 2019.

[7] M. De Lozzo and A. Marrel. New improvements in the use of dependence measures for sensitivity analysis and screening. Journal of Statistical Computation and Simulation, 86:3038-3058, 2016.

[8] F. Bachoc, G. Bois, J. Garnier, and J.M. Martinez. Calibration and improved prediction of computer models by universal Kriging. Nuclear Science and Engineering, 176:81-97, 2014.

[9] G. Damblin, M. Couplet, and B. Iooss. Numerical studies of space-filling designs: Optimization of latin hypercube samples and subprojection properties. Journal of Simulation, 7:276-289, 2013.

[10] E. Song, B. Nelson, and J. Staum. Shapley effects for global sensitivity analysis: Theory and computation. SIAM/ASA Journal on Uncertainty Quantification,4:1060-1083, 2016.

[11] J.O. Ramsey and B.W. Silverman. Functional Data Analysis. Springer, New York, 2005.